Investigation on Vibration of Amorphous Alloy Transformer Core

Daosheng Liu*, Peng Li, and Zeshuai Li

Abstract—Amorphous alloy transformers (AMDTs) have become the mainstream of energy-saving and environmentally friendly distribution transformers, but the problem of environmental pollution caused by their noise has become more prominent. The high magnetostriction of amorphous alloy strip and its sensitivity to stress are the main reasons for the vibration of AMDT core. Accurate calculation of the overall core vibration of transformers is the key issues in transformer noise research. This paper studies the vibration of amorphous alloy transformers under operating conditions and establishes a three-dimensional magnetic-mechanical coupling model considering the magnetostrictive effect of the power transformer core, and the magnetic field distribution and core vibration displacement of the dry-type transformer under no-load conditions are calculated by finite element method. Combined with experiments, the mechanism of vibration generation of amorphous alloy transformer core is studied, and an iron core vibration prediction calculation based on electromagnetic field coupling analysis is proposed. The research results not only have important academic value for exploring the vibration mechanism and noise suppression mechanism of amorphous alloy transformers, but also have significance for ensuring their efficient operation.

1. INTRODUCTION

As an indispensable power equipment in the power system, the transformer undertakes the functions of power transmission and voltage conversion, and it is the transit hub of power transmission. Although silicon steel sheets transformers have significantly improved material, electrical and structural properties, there has not been an effective solution to the problem of high loss caused by silicon steel sheet materials for transformer cores. Amorphous alloy distribution transformers (AMDTs) are distribution transformers whose iron cores are made of amorphous alloy strips. AMDTs are prepared by using amorphous alloy strips as iron core materials through a special process. After secondary annealing in a vertical magnetic field, the core loss value is the lowest value of the metal core, and its saturation induction B_s is slightly higher than 1.5 T. This material has a lower core loss [1]. The no-load loss and no-load current generated during operation are 25% and 20% of those of silicon steel sheet transformers, respectively [2, 3]. Their energy-saving effect makes them have broad application potential in the field of power transmission and distribution. In power distribution system, AMDTs are more and more widely used and have gradually replaced other types of transformers as the mainstream of energy-saving and environmentally friendly distribution transformers. The high magnetostriction and stress sensitivity of amorphous alloy materials make it impossible for better fixed confinement, which leads to high vibration and high noise of AMDT during operation. At present, there is no general mathematical model for AMDT core vibration.

Hu et al. carried out the electromagnetic field simulation calculation of the model and obtained the electromagnetic force distribution on the iron core and winding, then applied the electromagnetic force

Table 1. Definition of variables.

M	magnetization intensity
M_S	Saturation magnetization
M_{WS}	Saturated wall shift magnetization
$M(\sigma)$	Saturated wall displacement magnetization function related to stress
θ	the angle between each magnetic domain and magnetization direction
G	Elastic Gibbs free energy per unit volume
T	temperature
S	entropy density
U	internal energy per unit volume
σ	prestress
σ_S	the maximum prestress range of the simplified model
ε	strain
B	Magnetic induction intensity
E_S	proper Young's modulus
λ_s	Saturation magnetostriction coefficient
M_{ws}	Saturation wall shift magnetization
H	Magnetic field intensity

to the harmonic response analysis to obtain the vibration trend and displacement of each node of the iron core and winding [4].

Chen and other scholars [5] took the 160kVA single-phase two-frame three-column transformer core as the research object, carried out the electromagnetic-stress-sound field coupling analysis, and obtained the vibration amplitude characteristics of the core under the introduction of different DC biases.

The magnetostrictive effect is the main cause of the high noise of AMDT [7, 8], scholars first studied the magnetostrictive phenomenon of AMDT. Sato and Todaka studied the cause of the deterioration of the magnetic properties of the core due to magnetostriction [9]. Based on the vibration-acoustic coupling calculation, Zhang et al. obtained the damping coefficient of the transformer core vibration and conducted a magnetic-structure coupling analysis on the vibration of the transformer core to study the core vibration [10].

Based on the macro-thermodynamic relationship, combining with the micro-physical mechanism of prestress affecting the maximum value of magnetostrictive strain and its variation law, a one-dimensional calculation model that can reflect the magnetostrictive strain is established.

The specific research content of this paper is to establish a three-dimensional simulation model of the amorphous alloy transformer core, excite the excitation coil under no-load conditions, carry out the simulation calculation of the main magnetic flux, and obtain the distribution cloud map of the transformer core and the main magnetic flux. The vibration deformation of each position of the iron core is calculated by using the established prediction model. According to the calculation results, the actual complex situation of AMDT is fully considered to provide theoretical and technical support for the design and development of crystal alloy transformers [11–13].

Combined with the experimental situation, other factors of iron core vibration are considered on the basis of calculation, in order to accurately predict the vibration of each part of the AMDT core.

2. VIBRATION CALCULATION

2.1. Magnetostrictive Model of Amorphous Alloy Core

The research results [14–16] show that the source of the vibration of the transformer body is the vibration of the core caused by the magnetostriction of the strip. The vibration is the movement of the

magnetic domain and the rotation of the magnetic moment during the magnetization process, so that the volume of the amorphous alloy material changes. It is worth noting that when the amorphous alloy iron core is subjected to a certain prestress, the magnetic domain will be shifted due to the stress, and the magnetic domain will be shortened along the direction of the stress (stress anisotropy). Therefore, the magnetostriction of the iron core will change, but there is a complex nonlinear relationship between the prestress and the magnetostrictive strain [17–19].

The magnetization process of magnetic materials can be represented visually by mathematical formulas. When there is no external magnetic field, the direction of the magnetic moment of each magnetic domain is disordered, and the ferromagnetic material as a whole does not show magnetism. Choose a direction arbitrarily, and the angle between each magnetic domain and this direction is represented by θ. This process can be represented by the following formula.

$$\sum M_S V_i \cos \theta_i = 0 \tag{1}$$

There, V_i is the magnetic moments of magnetic domains, M_S the saturation magnetization, and θ the angle between each magnetic domain and magnetic field direction.

When an external magnetic field is applied to a magnetic material for magnetization, the movement of the domain wall and the rotation of the magnetic moment both play their part. The magnetic moment component per unit volume along the direction of the external magnetic field in the magnetized state is shown in ΔM_H:

$$\Delta M_H = M_S \left[\sum \cos \theta_i \Delta V_i + \sum V_i \Delta \left(\cos \theta_i \right) \right] \tag{2}$$

The AMDT core is subjected to a predetermined tensile and compressive stress and an external magnetic field in the axial direction, and the generated magnetization and output strain are also in the axial direction. Therefore, the constitutive model of the relationship can be simplified to a one-dimensional model.

Based on the macro-thermodynamic relationship, combined with the micro-physical mechanism of prestress affecting the maximum magnetostrictive strain and its variation law, a one-dimensional physical model that can reflect the vibrational deformation of amorphous alloys is established.

Defining the elastic Gibbs free energy per unit volume

$$\begin{cases} G\left(\sigma, M, T\right) = U - TS - \sigma\varepsilon \\ dT = 0 \end{cases} \tag{3}$$

There, T is the temperature, S the entropy density, U the internal energy per unit volume, σ the prestress, and ε the strain.

In order to obtain the constitutive relation in polynomial form, Taylor expansion is carried out with (3) in the natural state

$$G\left(\sigma, M\right) = G_0 + \frac{\partial G}{\partial \sigma}\sigma + \frac{1}{2}\frac{\partial^2 G}{\partial \sigma^2}\sigma^2 + \ldots + \frac{2}{2!}\frac{\partial^2 G}{\partial \sigma^2}\sigma M + \frac{3}{3!}\frac{\partial^3 G}{\partial \sigma \partial M^2}\sigma M^2 + \ldots + \frac{\partial G}{\partial M}M + \frac{1}{2}\frac{\partial^2 G}{\partial M^2}M^2 + \ldots \tag{4}$$

Since the elastic free energy G in the natural state is constant and has no contribution to the partial derivative, the stress, strain, magnetic field strength, and magnetization in the natural state are all zero. According to the experimental results of Kuruzar and Cullity [20] and the fitting formula of Jiles [21], only those terms containing M^2 and M^4 are retained in the coupling terms of Equation (4), and M^3 and M^5 can be simplified in Equation (4), so that we get Equation (5):

$$\begin{aligned} \varepsilon = {} & -\frac{\partial^2 G}{\partial \sigma^2}\sigma - \frac{1}{2}\frac{\partial^3 G}{\partial \sigma^3}\sigma^2 - \frac{1}{3!}\frac{\partial^4 G}{\partial \sigma^4}\sigma^3 - \ldots - \left(\frac{1}{2}\frac{\partial^3 G}{\partial \sigma \partial M^2} + \frac{1}{2}\frac{\partial^4 G}{\partial \sigma^2 \partial M^2}\delta + \frac{1}{4}\frac{\partial^5 G}{\partial \sigma^3 \partial M^2}\sigma^2 + \ldots\right)M^2 \\ & -\frac{1}{4!}\left(\frac{\partial^5 G}{\partial \sigma \partial M^4} + \frac{\partial^6 G}{\partial \sigma^2 \partial M^4}\sigma + \ldots\right)M^4 \end{aligned} \tag{5}$$

The constitutive relation in polynomial form is obtained. The change of the magnetic domain structure is the physical mechanism of magnetostriction. But for amorphous alloy magnetic materials, the effect of external stress will also affect the magnetic domain structure. The experimental measurement results show that the magnetostriction of the amorphous alloy iron core not only has

a strong nonlinear relationship with the magnetic field, but also is affected by various complex factors such as temperature and prestress, between which the effect of prestress is more important.

Stress will not only cause elastic deformation, but also affect the microscopic magnetic domain structure of the ferromagnetic material, causing it to generate pre-magnetostrictive strain. Therefore, there is a complex nonlinear relationship between stress and strain. According to the above analysis, this paper decomposes the elastic strain generated by the stress in the iron magnetic material into the sum of two parts: one is $\frac{\sigma}{E}$ which is not related to the migration of the magnetic bin wall. This part is linear and can be described by its inherently Young modulus E, and the other is $\lambda(\sigma)$ which can be described as a nonlinear function. In this way, the elastic strain type can be expressed as (6).

$$-\frac{\partial^2 G}{\partial \sigma^2}\sigma - \frac{1}{2}\frac{\partial^3 G}{\partial \sigma^3}\sigma^2 - \frac{1}{3!}\frac{\partial^4 G}{\partial \sigma^4}\sigma^3 - \ldots = \frac{\sigma}{E} + \lambda(\sigma) \tag{6}$$

$\frac{\sigma}{E}$ stands for the elastic strain, and $\lambda(\sigma)$ represents the magnetostrictive strain caused by prestressing.

Simultaneously solve (5) and (6) to get the magnetostrictive deformation formula of AMDT core.

$$
\begin{aligned}
\varepsilon &= \frac{\sigma}{E_S} + \lambda(\sigma) + \frac{\lambda_S - \lambda(\sigma)}{M_{ws}^2}M^2 - \frac{\theta\lambda_S}{M_{ws}^4}\left(M^4 - M(\sigma)^4\right) \\
H &= \frac{1}{k}f^{-1}\left(\frac{M}{M_S}\right) - \frac{2(\lambda_S\sigma - \Lambda_0(\sigma))}{\mu_0 M_{ws}^2}M + \frac{4\theta\lambda_s\sigma}{\mu_0 M_{ws}^4}\left(M^3 - M(\sigma)^3\right)
\end{aligned}
\tag{7}
$$

There, the function $M(\sigma)$ represents the variation of saturation wall-shift magnetization with stress. $f(\sigma)$ describes the magnetization curve of the free state. E_S is the Young's modulus, and k is the relaxation factor. M_{ws} is the saturation wall shift magnetization, λ_s the saturation magnetostriction coefficient, and $\Lambda_0(\sigma) = \int_0^{\sigma}\lambda_0(\sigma)d\sigma$. H is the magnetic field intensity. Due to the introduction of the step function, the third term of magnetization actually starts from $M_0(\sigma)$. Therefore, the corresponding part of saturation wall-shifting magnetization must be removed from the magnetization. Only in this way can we ensure that the magnetization curve does not show a jump at the saturation wall-shifting magnetization, but changes continuously.

In the above (7) there are three function unknowns $M(\sigma)$, $\lambda(\sigma)$, and $f(\sigma)$.

2.2. Simplify the Unknown Function

For $\lambda(\sigma)$, although its precise expression is usually difficult to get, its main characteristics can still be obtained from the stress-strain curve in the demagnetized state. Jiles [21] fitted the experimental data and obtained:

$$\lambda = \left[7 \times 10^{-18} - 1 \times 10^{-25}\delta\right]M^2 + \left[-3.3 \times 10^{-30} + 2.1 \times 10^{-38}\delta\right]M^4 \tag{8}$$

Therefore, the coefficients in Equation (7) in front of the square and quartic terms are linear functions of stress.

Under the action of prestress σ, the domain wall shift will lead to nonlinear strain, so that the maximum magnetostrictive strain becomes $M_{\max}(\sigma) = M_S - M_0(\sigma)$ when saturation wall-shift magnetization is reached in the external magnetic field. From the perspective of magnetic domain analysis, under prestress σ, the variation of saturation wall shift magnetization $M(\sigma)$ and the maximum magnetostrictive strain with stress are both caused by the magnetic domain wall shift, and their mechanisms are the same from the microscopic perspective. Therefore, the saturated wall-shifted magnetization $M(\sigma)$ should also be equal to the difference between the saturated wall-shifted magnetization M in the free state and the nonlinear "pre-magnetization" under the above prestress. Therefore, the saturated wall-shifted magnetization under the prestress has the same expression as the maximum magnetostrictive strain under the stress, with different coefficients. Its specific expression can be taken as;

$$M(\sigma) = M_{WS}\left(1 - \tanh\left(\frac{\sigma}{\sigma_s}\right)\right) \tag{9}$$

There, M_{WS} is the saturated wall shift magnetization, and δ_s is the maximum prestress range of the simplified model. The linearity of stress-strain is true only for small stresses. Therefore, the simplified

model can only be applied when the stress is small. If the stress orifice is very large, there will be not only a large quantitative error, but also a physically impossible result.

For the nonlinear function $f(\sigma)$ describing the magnetization curve of the free state, the LANGEVIN function is selected for simplification, where k is the relaxation factor.

$$\begin{cases} M = M_S \left[\coth{(kH)} - \dfrac{1}{kH} \right] \\ k = \dfrac{3\sigma_s}{M_s} \end{cases} \tag{10}$$

2.3. Model Finite Element Calculation

The research object of this paper is SCBH15-200/10 dry-type amorphous alloy transformer. The iron core is made of amorphous alloy material by stepping lap method. The single-phase iron core is composed of a large-frame iron core and a small-frame iron core. The iron core model is shown in Fig. 1.
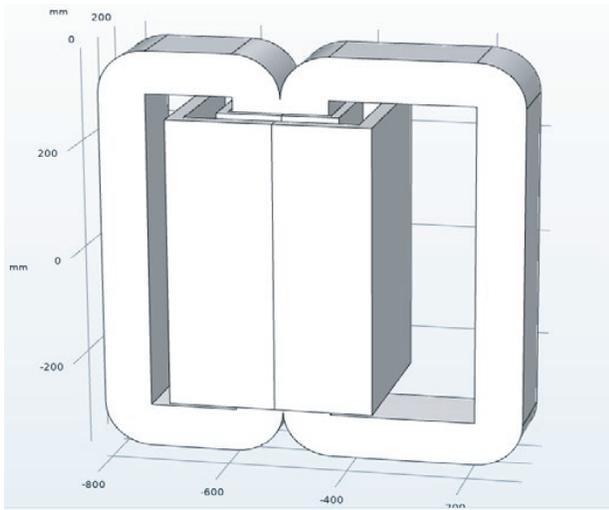
Figure 1. Core geometry.
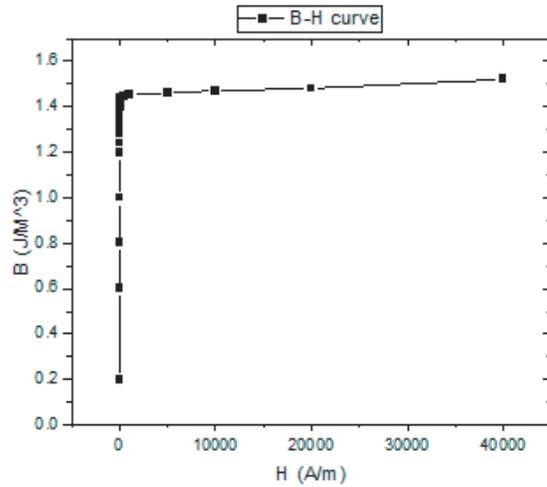
Figure 2. Core material B-H curve.

In the model: the thicknesses of the upper iron yoke and the left and right iron yokes are the same; the thickness of the lower iron yoke is 1.18 times the thickness of the upper iron yoke; the height of the iron core window is 590 mm; the width of the small frame iron core window is 145 mm; the width of the large frame iron core window is 240 mm; the thickness is 79.5 mm; the width of the amorphous alloy strip is 142.24 mm.

The B-H curve is used to describe the magnetization process of the iron core material. The B-H curve of the SCBH15-200/10 iron core is shown in Fig. 2.

In finite element calculations, if the mesh is too finely divided, the computational complexity will increase, and it will take a lot of time to obtain the calculation results; if each mesh is relatively coarsely divided, the calculation accuracy will not meet the requirements, resulting in deviations between the simulation results and actual values. In order to balance the contradiction between the solution accuracy and the amount of calculation, when meshing the model in this paper, this paper uses an ultra-coarse mesh evenly to divide the regular areas outside the iron core and windings. For the irregular areas of the iron core and windings using a more refined division method, the division results are shown in Fig. 3.

When carrying on the FEM (finite element calculation) of electromagnetic field, the mathematical model of amorphous alloy material of magnetic induction intensity deduced in Section 2 is set as the constitutive relationship of FEM.
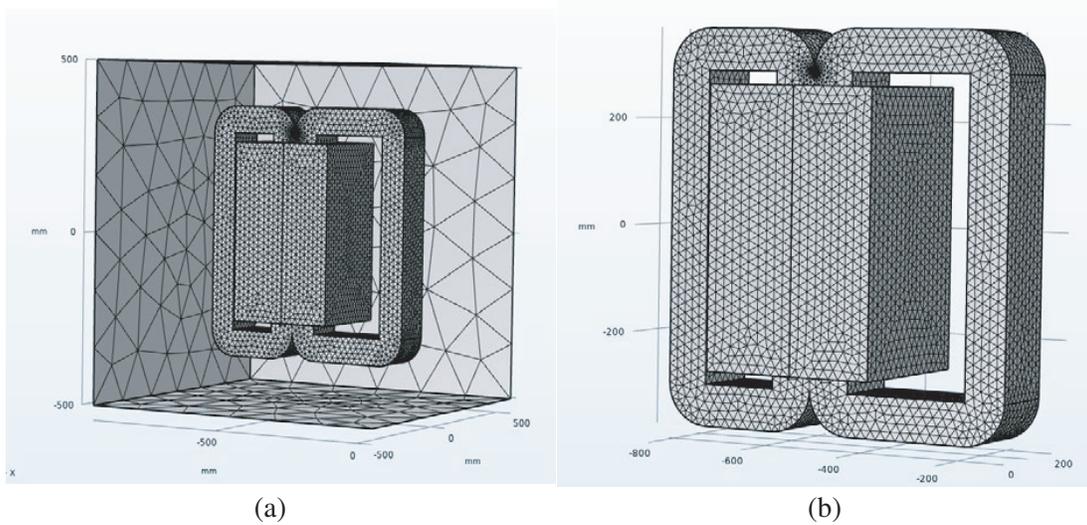
Figure 3. Grid model.

The AMDT main magnetic flux density distribution of the core is shown in Fig. 4. It can be seen that the maximum magnetic flux density of the core is 1.4 T, and the average magnetic flux density is 1.337 T, which is consistent with previous research conclusions and also verifies the correctness of formula (7). There is a significantly higher flux density at the inner corner of the core, which means that magnetostriction is greater here than elsewhere. This is because the magnetic field lines of the iron core converge here, as shown in Fig. 5. The distribution of magnetic flux density can help determine the signal collection point of the test.
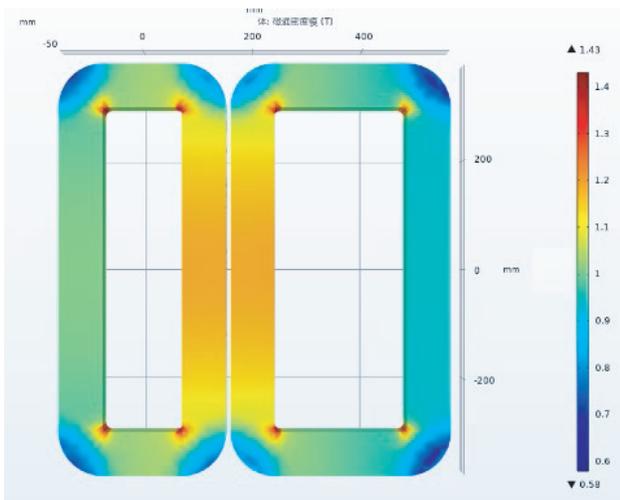
Figure 4. Core main magnetic flux density.
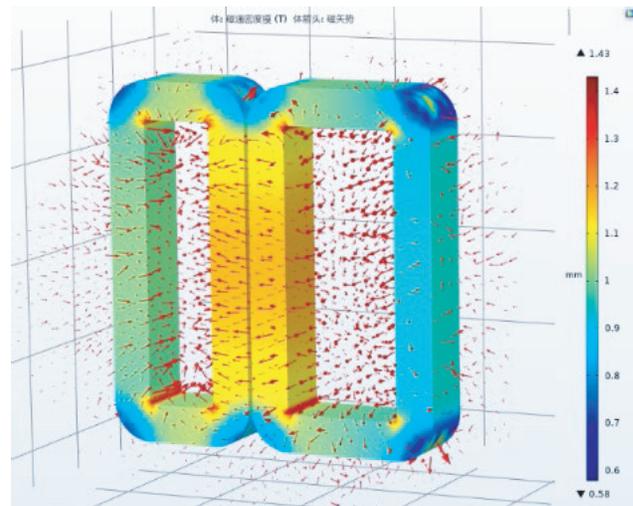
Figure 5. Magnetic vector distribution.

In addition, the distribution of the leakage flux between the iron core and the winding is shown in Fig. 6. It can be seen from Fig. 6 that the maximum density of the leakage flux is concentrated on the chamfer edge of the iron core, and the value is only 0.001 T. It is known that the magnetic flux density of the iron core is closely related to its magnetostrictive deformation, so the influence of the leakage flux can be ignored in subsequent calculations.

The results of the FEM of the above electromagnetic field are used as the acceleration excitation
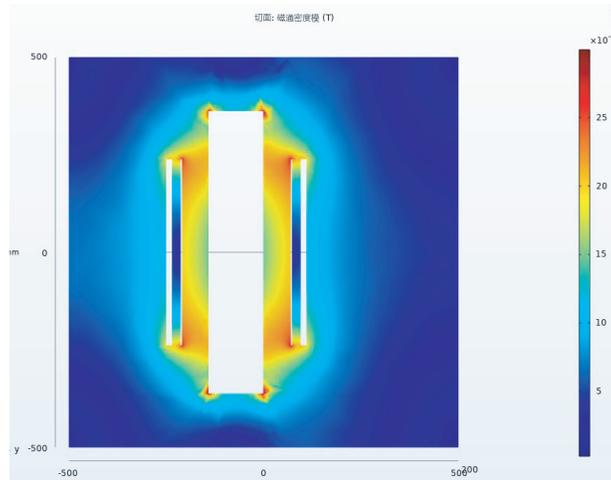
Figure 6. Magnetic flux density distribution of leakage magnetic field.
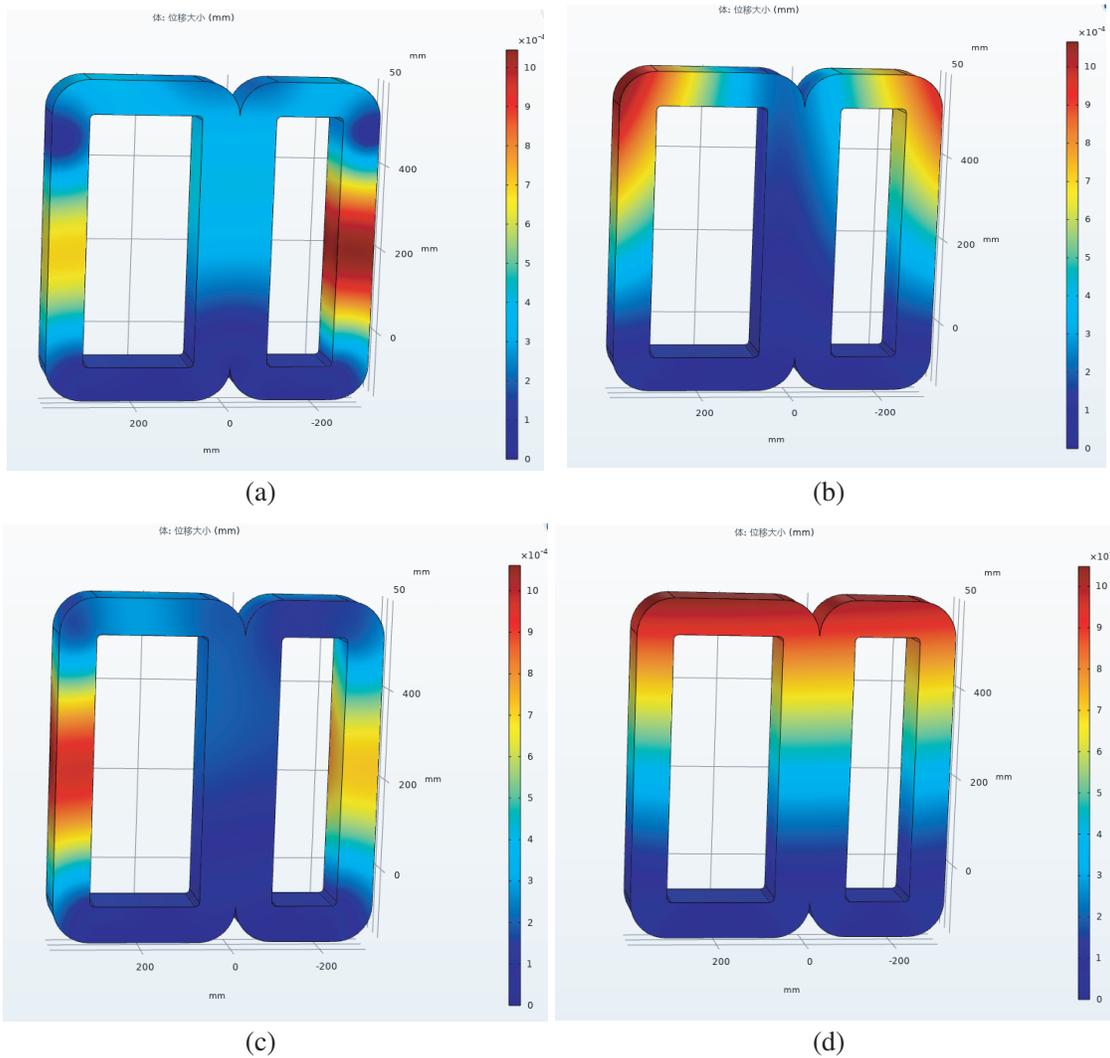
Figure 7. Magnetostrictive deformation of core at different times. (a) 2 ms. (b) 4 ms. (c) 6 ms. (d) 8 ms.

input of the structure field, and the deformation results of the iron core at different times are obtained through the calculation of the polynomial constitutive relation of the magnetostrictive deformation, as shown in Fig. 7.

When an alternating voltage is applied, an alternating magnetic flux is generated in the iron core. The magnetostrictive deformation obtained by the finite element calculation of the polynomial constitutive relation established in this paper is shown in Fig. 7. As can be seen from the figure, due to the change of the magnetic flux, the deformation position of the iron core will also change accordingly. The data obtained by the finite element calculation is compared with the experimental data to verify the model in this paper.

3. EXPERIMENTAL VERIFICATION

The multi-channel vibration test is shown in Fig. 8, and the AMDT SBH15-10-10/0.4 is used as the experimental target [22]. During the test, the influence of high and low voltage copper bar and core insulation coating on magnetic flux density is ignored, so only the excitation is applied to the coil unit. When the excitation is applied, the given excitation is carried out on the side of the high-voltage winding. Since the rated number of turns of the high-voltage winding is 953, the rated current of each turn is 6.67 A. The voltage regulator is used to obtain the stability of the AC voltage and the holding voltage, and the ICP Vibration sensors are used to monitor the vibration signals on the surface of the AMDT fuel tank and the surface of the upper clamp.
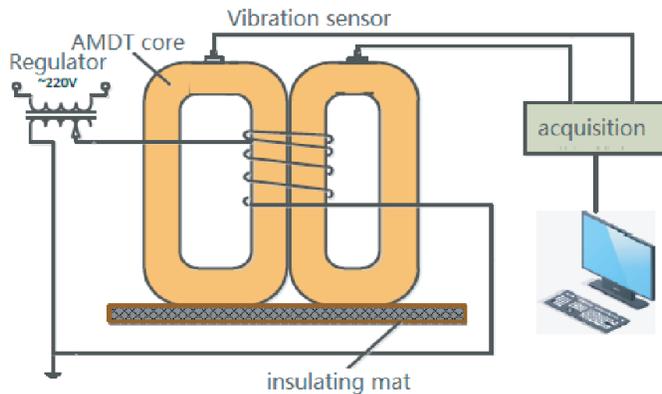
Figure 8. The multi-channel vibration test.
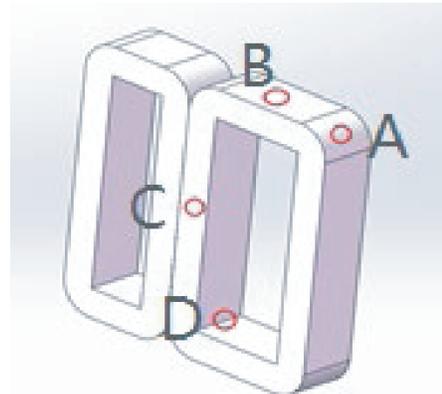
Figure 9. Sensor collection location.

According to the above calculations and descriptions, the vibration energy is the largest at the inner chamfer of the iron core, and a sensor is placed at D to collect the core vibration. For comparison, a sensor is also placed at A, the outer corner of the iron core. Because the magnetic flux density and vibration energy distribution of the upper yoke and the core are relatively uniform, the sensor is placed in their middle position to verify the weak vibration at this position. The overall arrangement of the sensor on the iron core is shown in Fig. 9 and Figs. 11–12.

The test system in the figure consists of two parts: a data acquisition unit and a data processing unit. One part consists of an ICP vibration sensor, and the other part consists of an A/D acquisition card and a computer, shown in Fig. 10.

The vibration signal of the transformer core and related parts is an electrical and mechanical vibration signal. The vibration frequency bandwidth is $10 \sim 2000$ Hz, and the amplitude is between $0.5 \sim 500\,\mu$m. The object of this research is an amorphous alloy transformer designed according to the principle of electromagnetic induction, which has strong electromagnetic field interference in working or experimental conditions; in addition, this research needs to measure the vibration signal on the surface of the object, and the displacement sensor cannot be pasted on the surface of the test object, so accelerometers are ideal for transformer vibration measurement systems.

Figure 10. A/D acquisition card.

Figure 11. Experimental A B measuring points.

Figure 12. Experimental C D measuring points.

400 V voltage is applied to the excitation coil, and vibration and noise signals are collected by sensors. During the experiment, the PC recorded the vibration characteristics, and the noise meter recorded the sound pressure level. In order to obtain all smooth waveforms and frequency components after Fast Fourier (FFT) spectral analysis, the sampling frequency was selected as 32 kHz.

Compared with the related research conclusions of Chen et al. [23], the complex magnetostrictive constitutive relationship of amorphous alloys is dealt with by constructing one-dimensional constitutive relationship from the energy perspective, which can be easier to predict the magnetic telescopic expansion of amorphous alloys deformation.

The experimental results show that the vibration signal is periodic; the vibration frequency is concentrated in $0 \sim 600\,\text{Hz}$; and the vibration frequency of the iron core is an integer multiple of $100\,\text{Hz}$. Magnetostrictive nonlinearity will result in higher harmonic frequency content. When the frequency is greater than $600\,\text{Hz}$, the vibration amplitude is close to zero.

Figures 13–16 show that the core vibration frequency is an integer multiple of $100\,\text{Hz}$, which is consistent with the previous description that the core vibration fundamental frequency is twice of that of the power supply, proving the correctness of the experimental signal acquisition and data processing. When the frequency is from $100\,\text{Hz}$ to $600\,\text{Hz}$, the vibration amplitude decreases gradually, and the
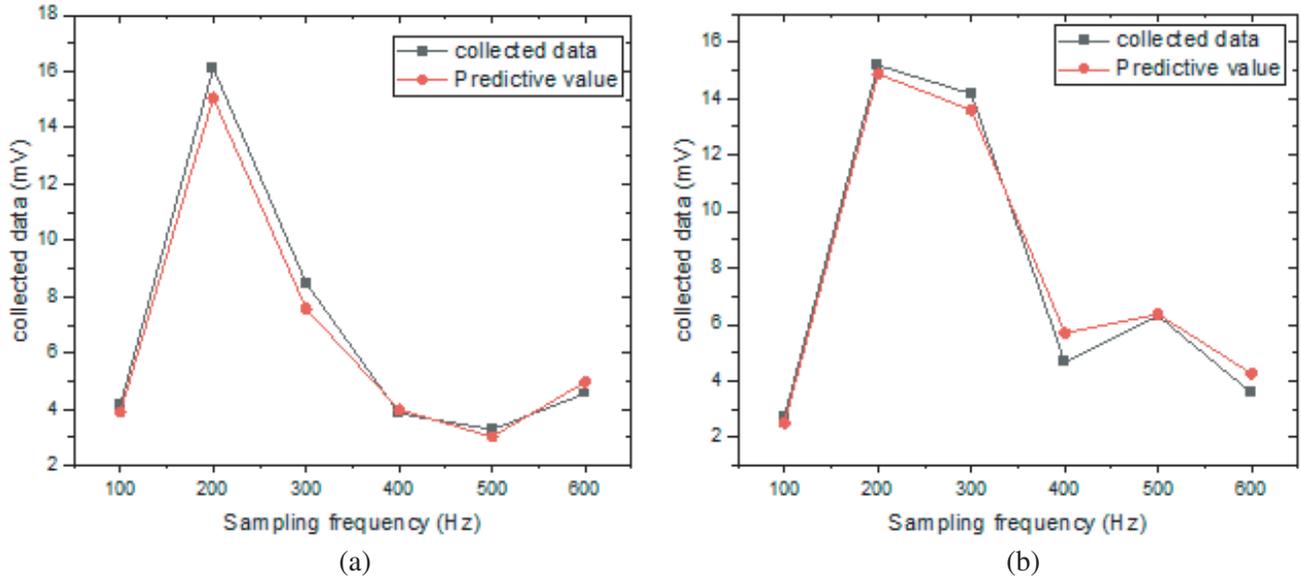
Figure 13. Comparison results at A. (a) Unconstrained iron core. (b) Iron core with fixed restraint of upper jaw.
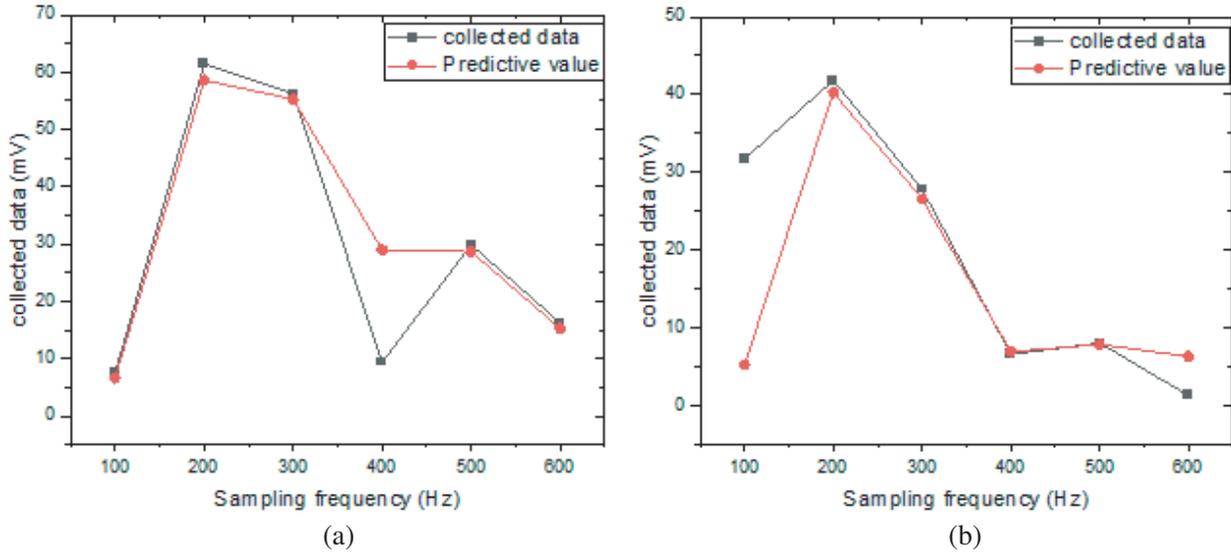
Figure 14. Comparison results at B. (a) Unconstrained iron core. (b) Iron core with fixed restraint of upper jaw.

contribution to vibration is the least, which can be approximately ignored. At the same time, the vibration amplitude reaches the maximum when the frequency is 200 Hz, which is caused by the fact that the amorphous alloy core cannot be fully clamped by external forces during the assembly process. Therefore, the resonance phenomenon at 200 Hz should be avoided.

The results show that the vibration amplitude is the largest at the inner chamfer of the iron core made of amorphous alloy, and the vibration deformation is larger at 200 Hz when there is no fixed constraint. There is a large difference between the calculated values and experimental data at individual frequencies, such as 400 Hz at B point and 600 Hz at D point. This phenomenon is mainly because the theoretical model in this paper is constructed based on the constitutive relationship of
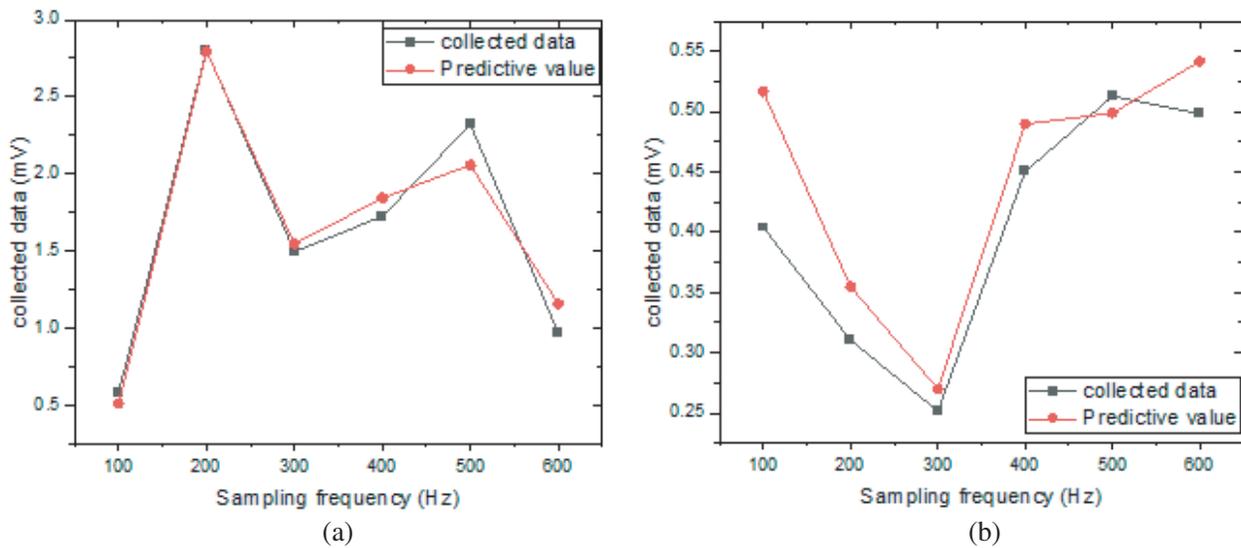
Figure 15. Comparison results at C. (a) Unconstrained iron core. (b) Iron core with fixed restraint of upper jaw.
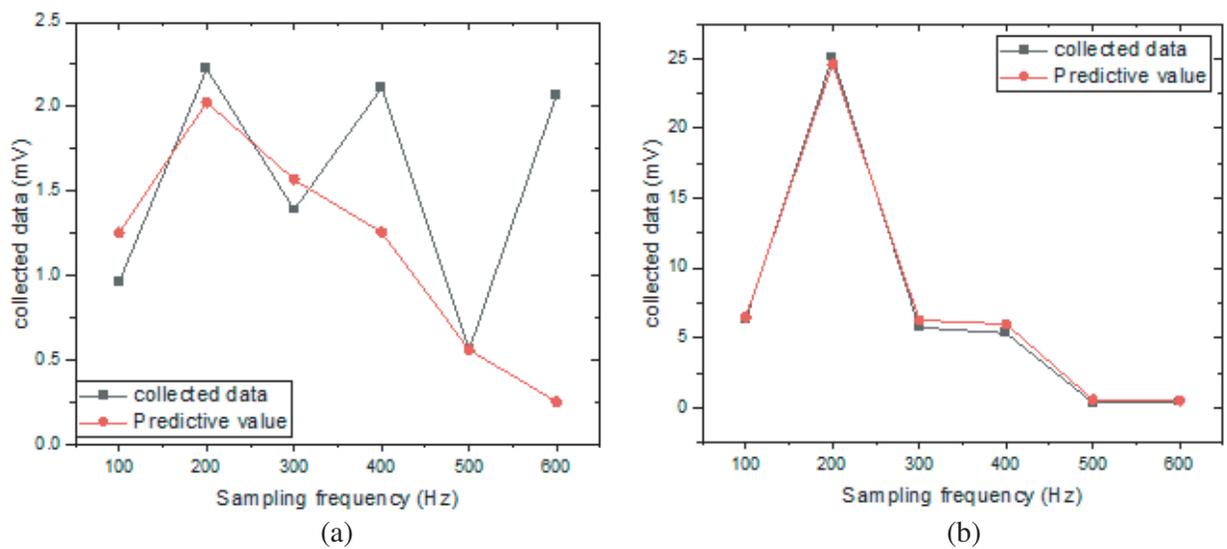
Figure 16. Comparison results at D. (a) Unconstrained iron core. (b) Iron core with fixed restraint of upper jaw.

the magnetostriction of amorphous alloys, and the vibration deformation of the transformer core is the result of a variety of factors. Geometry and frequency characteristics of core are both play their part.

The modal analysis of the transformer core in this experiment shows that at 400 Hz, the upper jaw of the core will have a large up and down vibration deformation, which leads to the fact that the vibration data at point B at 400 Hz in the experiment is much larger than that calculated by the model result. Similarly, at point D, the core will have a large back and forth swing deformation at 600 Hz, and the vibration deformation of point D will increase when the core lacks restraint. After imposing a certain fixed constraint on the outer chamfer of the iron core to limit its swing, it can be found in Fig. 16(b) that the experimentally measured vibration data at point D coincides with the calculation results of the model in this paper to a high degree.

4. CONCLUSION

The vibration and noise characteristics on the AMDT cores have been surveyed, and a prediction calculation method is proposed for the vibration prediction of each part of the AMDT iron core due to magnetostriction. The following main conclusions can be obtained.

1) In this paper, the one-dimensional mathematical model based on magnetostriction can easily calculate the vibration deformation of amorphous alloy iron core caused by magnetostriction, which has certain value for transformer vibration research. The mathematical model of this paper only considers the influence of external force, and the cause is the comprehensive influence of many aspects.

2) AMDT core will aggravate vibration when there is no constraint. To reduce the vibration of AMDT iron core, it is necessary to impose different constraints on different parts or improve the structural design of the core according to its natural frequency.

ACKNOWLEDGMENT

REFERENCES

1. Luciano, B. A., et al., "Performance of single wire earth return transformers with amorphous alloy core in a rural electric energy distribution system," *Materials Research*, Vol. 15, 801–804, May 2012.
2. Roginskaya, L., Z. Yalalova, A. Gorbunov, and J. Rakhmanova, "Features of amorphous steel magnetic cores for transformers operating at mains frequency," *2020 International Conference on Electrotechnical Complexes and Systems (ICOECS)*, 1–5, Oct. 2020.
3. Yabu, N., K. Sugimura, M. Sonehara, and T. Sato, "Fabrication and evaluation of composite magnetic core using iron-based amorphous alloy powder with different particle size distributions," *IEEE Transactions on Magnetics*, Vol. 54, 1–5, Nov. 2018.
4. Hu, J. Z., D. Liu, Q. F. Liao, et al., "Analysis of transformer electromagnetic vibration and noise based on finite element method," *Journal of Electrotechnical Technology*, Vol. 31, 81–88, 2016.
5. Chen, D. Z., B. Q. Hou, Z. Y. Feng, and B. D. Bai, "Study of magnetostriction influence of electrical sheet steel under different DC biases," *IEEE Transactions on Magnetics*, Vol. 55, 1–5, Feb. 2019.
6. Liu, D. S., J. C. Li, et al., "Magnetic properties and vibration characteristics of amorphous alloy strip and its combination," *IET Electric Power Applications*, Vol. 13, 1589–1597, 2019.
7. Zhang, Y., Q. Li, D. Zhang, B. Bai, D. Xie, and C.-S. Koh, "Magnetostriction of silicon steel sheets under different magnetization conditions," *IEEE Transactions on Magnetics*, Vol. 52, 1–4, Mar. 2016.
8. Ohta, M. and R. Hasegawa, "Soft magnetic properties of magnetic cores assembled with a high Fe-based nanocrystalline alloy," *IEEE Transactions on Magnetics*, Vol. 53, 1–5, Feb. 2017.
9. Sato, T. and T. Todaka, "Effect of magnetic annealing on magnetic characteristic of amorphous wound core," *IEEE Transactions on Magnetics*, Vol. 54, 1–4, Nov. 2018.
10. Zhang, B., N. Yan, J. Du, F. Han, and H. Wang, "A novel approach to investigate the core vibration in power transformers," *IEEE Transactions on Magnetics*, Vol. 54, 1–4, Nov. 2018.
11. Chang, Y., C. Hsu, H. Chu, and C. Tseng, "Magnetomechanical vibrations of three-phase three-leg transformer with different amorphous-cored structures," *IEEE Transactions on Magnetics*, Vol. 47, 2780–2783, Oct. 2011.
12. Zhu, L., Q. Yang, R. Yan, X. Zhang, and Y. Yang, "Research on dynamic vibration of transformer with wireless power transfer system load," *IEEE Transactions on Magnetics*, Vol. 51, 1–4, Nov. 2015.
13. Ji, S. C., Y. F. Luo, and Y. Li, "Research on extraction technique of transformer core fundamental frequency vibration based on OLCM," *IEEE Transactions on Power Delivery*, Vol. 21, 1981–1988, Oct. 2006.

14. Tanzer, T., et al., "Magnetostriction of electrical steel and its relation to the no-load noise of power transformers," *IEEE Transactions on Industry Applications*, Vol. 54, 4306–4314, Sept.–Oct. 2018.

15. Moses, A., "Measurement of magnetostriction and vibration with regard to transformer noise," *IEEE Transactions on Magnetics*, Vol. 10, 154–156, Jun. 1974.

16. He, J., Z. Yu, R. Zeng, and B. Zhang, "Vibration and audible noise characteristics of AC transformer caused by HVDC system under monopole operation," *IEEE Transactions on Power Delivery*, Vol. 27, 1835–1842, Oct. 2012.

17. Rauschr, M., M. Kaltenbacher, H. Landes, et al., "Combination of finite and boundary element methods in investigation and predication of load-controlled noise of power transformer," *Journal of Sound and Vibration*, Vol. 250, 323–338, 2002.

18. Ji, S. C., Y. He, Y. M. Li, et al., "Research on vibration characteristics of power transformers under no-load conditions," *High Voltage Technology*, Vol. 05, 47–48, 2001.

19. Du, B. X. and D. S. Liu, "Dynamic behavior of magnetostriction-induced vibration and noise of amorphous alloy cores," *IEEE Transactions on Magnetics*, Vol. 51, 1–8, Apr. 2015.

20. Kuruzar, M. E. and B. D. Cullity, "The magnetostriction of iron under tensile and compressive stress," *International Journal of Magnetism*, Vol. 01, 323–325, 1971.

21. Jiles, D. C., "Theory of magnetomechanical effect," *J. Phys. D: Appl. Phys.*, Vol. 28, 1537–1546, 1995.

22. Takahashi, K., D. Azuma, and R. Hasegawa, "Acoustic and soft magnetic properties in amorphous alloy-based distribution transformer cores," *IEEE Transactions on Magnetics*, Vol. 49, No. 7, 4001–4004, Jul. 2013.

23. Chen, D., B. Hou, Z. Feng, and B. Bai, "Study of magnetostriction influence of electrical sheet steel under different DC biases," *IEEE Transactions on Magnetics*, Vol. 55, No. 2, 1–5, Art No. 2001305, Feb. 2019.